SUPPLEMENTAL DATA

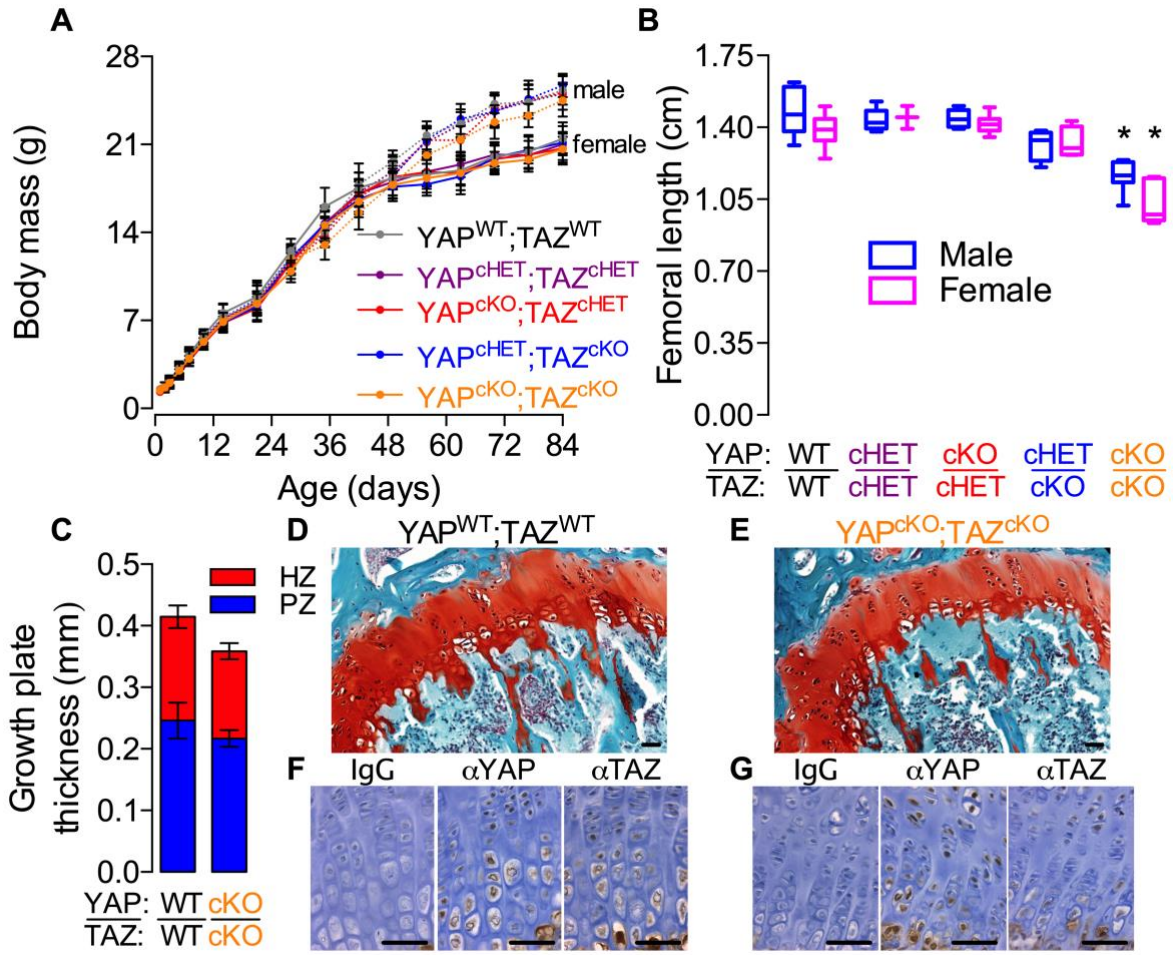

Supplemental Fig. 1. Combinatorial YAP/TAZ ablation with 8kb-DMP1-Cre is functionally redundant and does not recombine in growth plate chondrocytes. A) Body masses from mice with allele-dose dependent YAP/TAZ ablation from DMP1-expressing cells until P84. **B)** Femoral lengths from mice with allele-dose dependent YAP/TAZ ablation from DMP1-expressing cells at P84 for both males and females. **C)** Histomorphometric quantification of P84 growth plate thickness. HZ = hypertrophic zone. PZ = proliferating zone. **D)** Representative micrograph of P84 wild type ($YAP^{WT};TAZ^{WT}$) growth plate. **E)** Representative micrograph of P84 conditional double knockout ($YAP^{cKO};TAZ^{cKO}$) growth plate. **F)** Representative micrographs of chondrocyte immunostaining for IgG control, YAP, and TAZ in $YAP^{WT};TAZ^{WT}$ femurs at P28. **G)** Representative micrographs of growth plate chondrocyte immunostaining for IgG control, YAP, and TAZ in $YAP^{cKO};TAZ^{cKO}$ femurs at P28. Body mass data presented as mean with lines corresponding to the standard error of the mean (SEM). Sample sizes, N = 6-22 per sex per group. Femoral length data presented as a box and whiskers plots with whiskers corresponding to maximum and minimum values. Sample sizes, N = 2-10 per sex per group. Growth plate thickness percentage data presented as bars with lines corresponding to the mean and standard error of the mean (SEM). Sample sizes, N = 6 per group. Scale bars equal 50 μm in all images.

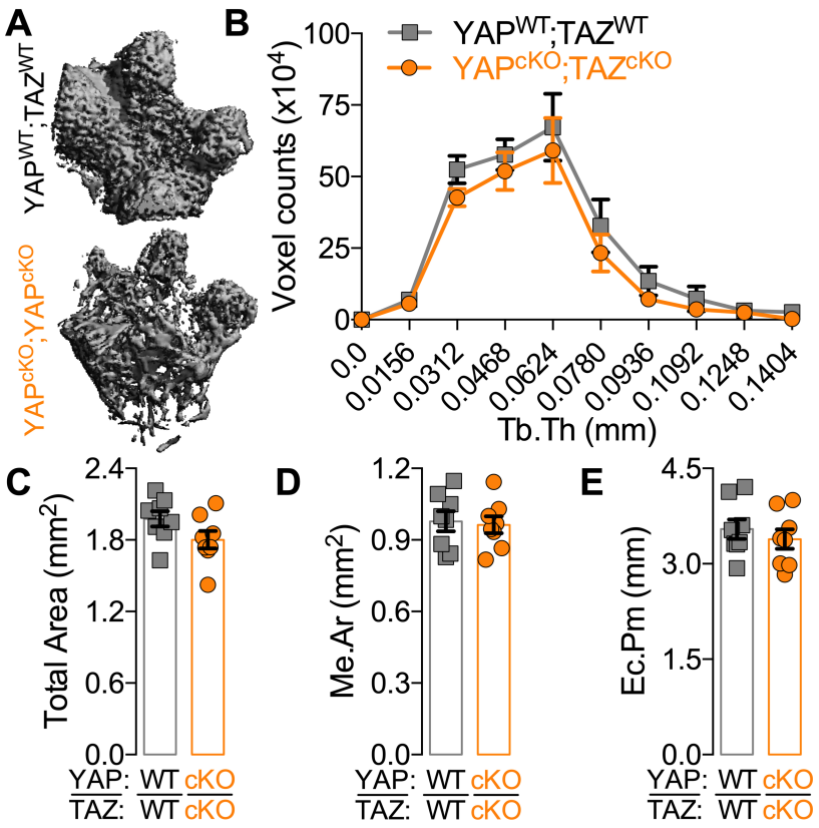

Supplemental Fig. 2. YAP/TAZ ablation from DMP1-expressing cells altered bone microarchitecture. A) Representative microCT reconstructions of distal metaphyseal microarchitecture in P84 femurs. **B)** Quantification of trabecular thickness distributions in cancellous bone. **C-E)** Quantification of cortical microarchitectural properties: **(C)** total area, **(D)** medullary area (Me.Ar), and **(E)** endocortical perimeter (Ec.Pm). Data are presented as bars and individual samples with lines corresponding to the mean and standard error of the mean (SEM). Sample sizes, N = 8 per group.

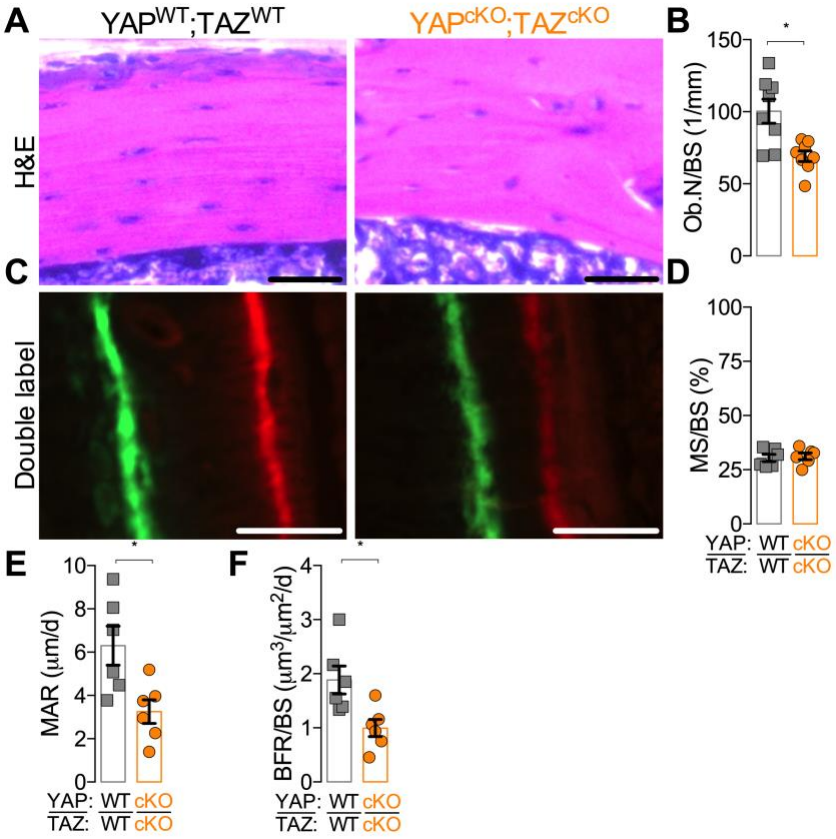

Supplemental Fig. 3. YAP/TAZ ablation from DMP1-expressing cells altered cortical osteoblast number and function. A) Representative micrographs of P84 cancellous metaphyseal bone stained by H+E. **B)** Quantification of osteoblast number per bone surface (Ob.N/BS). **C)** Representative micrographs of double flourochrome labeled cortical bone in P28 femurs. **D-F)** Quantification of **(D)** mineralizing surface percentage (MS/BS), **(E)** mineral apposition rate (MAR) and **(F)** bone formation rate (BFR/BS). Data are presented as bars and individual samples with lines corresponding to the mean and standard error of the mean (SEM). Sample sizes N = 6-8. Scale bars indicate 50 μm in all images.

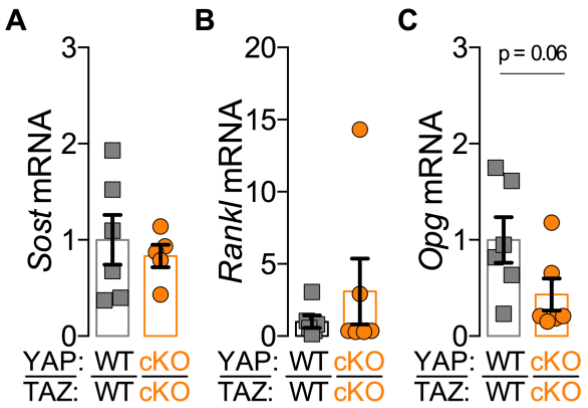

Supplemental Fig. 4. YAP/TAZ ablation from DMP1-expressing cells did not affect bone turnover markers. A-C) Femoral bone preparations from P84 mice were harvested to quantify mRNA expression. Expression levels, normalized to *18S rRNA*, were evaluated for **(A)** sclerostin (*Sost*), **(B)** receptor activator of nuclear factor kappa-B ligand (*Rankl*), and **(C)** osteoprotegerin (*Opg*), Data are presented as bars and individual samples with lines corresponding to the mean and standard error of the mean (SEM). Sample sizes, N = 5-6 per group.

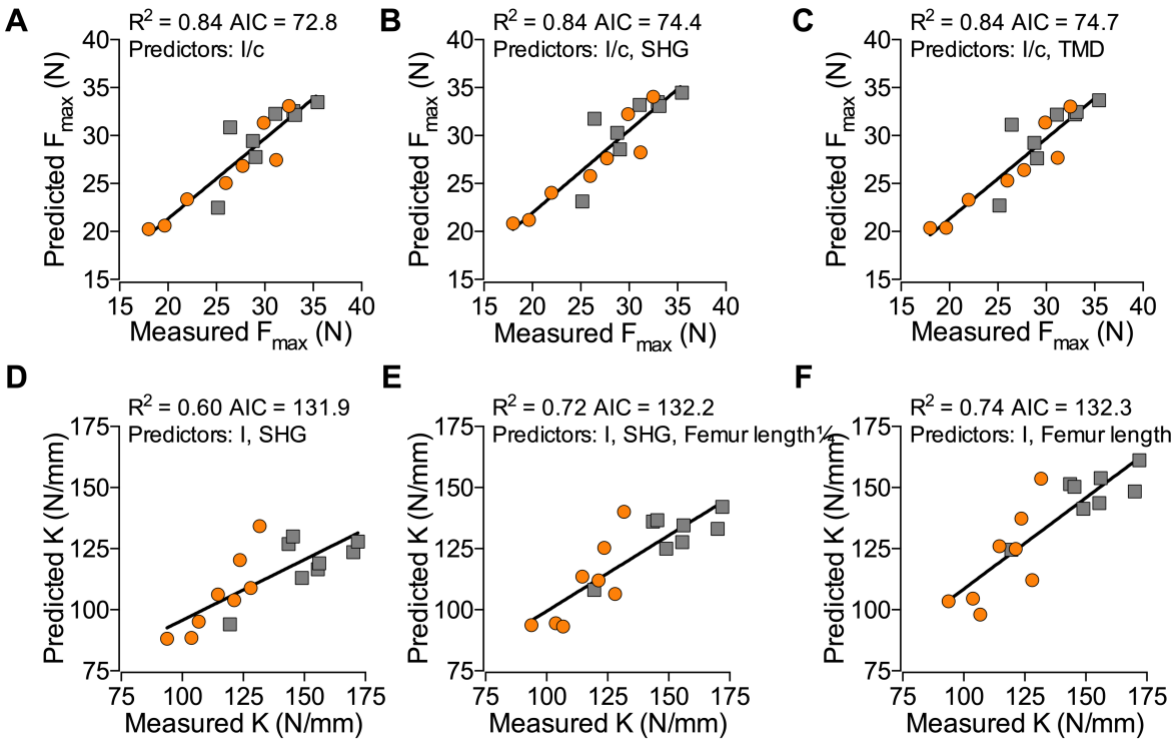

Supplemental Fig. 5. Best subsets analysis on morphological parameters from YAP/TAZ ablation in DMP1-expressing cells demonstrated increased goodness of fit for stiffness by accounting for collagen content and organization. Using the femurs that were scanned by microCT, tested in three-point bending, and imaged using SHG, experimental ultimate load (F_{max}) values were compared with predicted values from the top three "best" multivariate models in order from left to right. Models were ranked based on their relative Akaike's information criterion (AIC) value with the lowest AIC being the "best." The three "best" multivariate models for ultimate load were **A**) only section modulus (I/c), (**B**) I/c and second harmonic generated signal intensity (SHG), and (**C**) I/c and tissue mineral density (TMD) as a predictors. Similarly, (K) were (**D**) moment of inertia (I) and SHG, (**E**) I, SHG and femur length, and (**C**) I and femur length as predictors. Sample sizes, N = 8 per group.

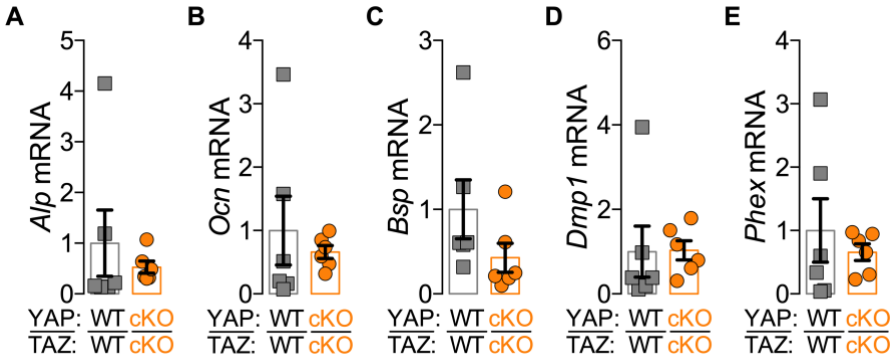

Supplemental Fig. 6. YAP/TAZ deletion did not alter osteogenic or osteocyte-marker gene expression. A-E) Femoral bone preparations from P84 mice were harvested to quantify mRNA expression. Expression levels, normalized to *18S rRNA*, were evaluated for **(A)** alkaline phosphatase (*Alp*), **(B)** osteocalcin (*Ocn*)**, (C)** bone sialoprotein (*Bsp*), **(D)** dentin matrix protein 1 (*Dmp1*), and **(E)** phosphate-regulating neutral endopeptidase (*Phex*). Data are presented as bars and individual samples with lines corresponding to the mean and standard error of the mean (SEM). Sample sizes, N = 6 per group.

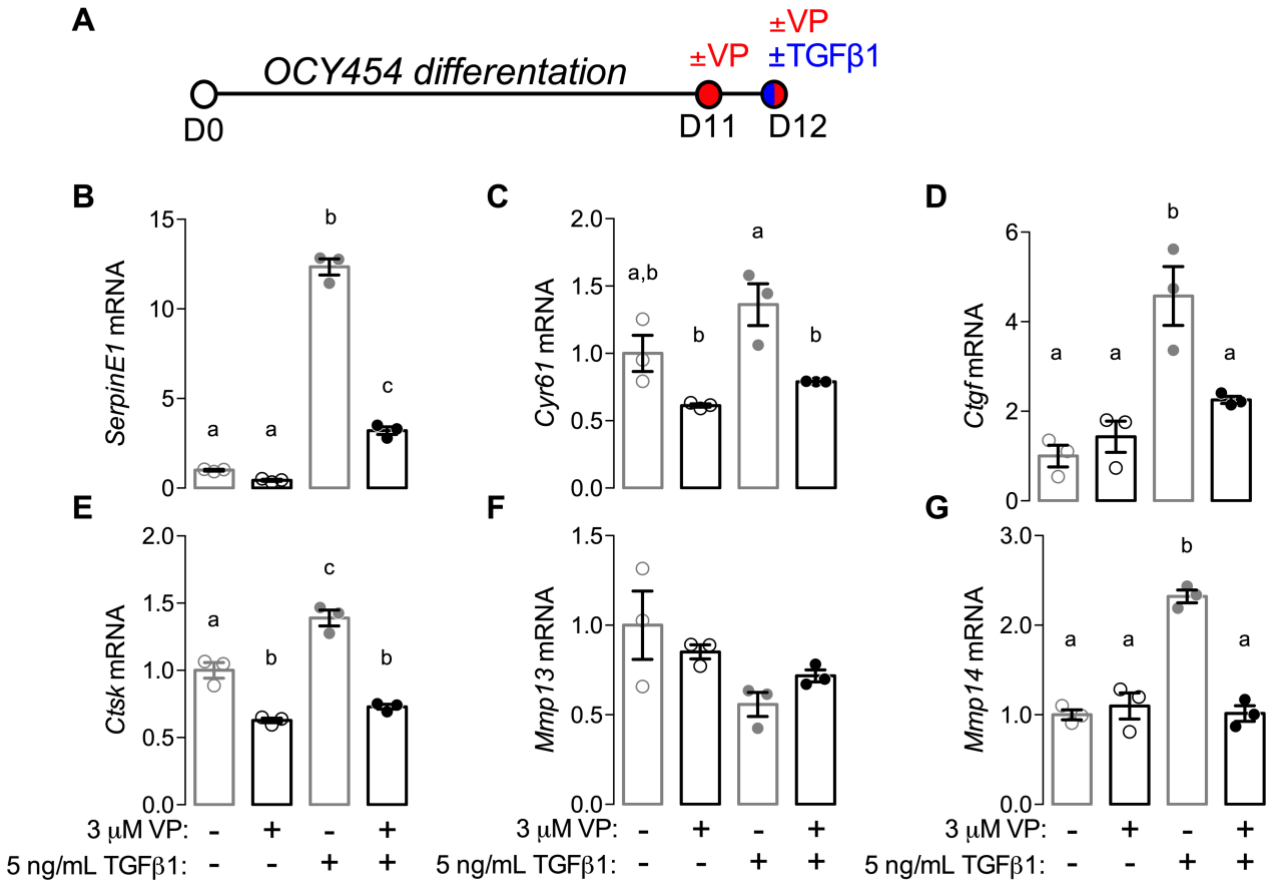

Supplemental Fig. 7. Inhibition of YAP/TAZ-TEAD with verteporfin (VP) reduced TGF-β-induced remodeling gene expression in OCY454 cells. A) Osteocyte-like cells, OCY454, were differentiated for 12 days. Cells were combinatorially treated with inhibitor verteporfin (VP) and 5 ng/ml TGF-β1 at day 12. **B-G)** mRNA expression, normalized to *18S rRNA*, was evaluated for **(B)** serpin family E member 1 (*SerpinE1*), **(C)** cysteine-rich angiogenic inducer 61 (*Cyr61*), **(D)** connective tissue growth factor (*Ctgf*), **(E)** cathepsin K **(***Ctsk*), **(F)** matrix metalloproteinase-13 (*Mmp13*), and **(G)** matrix metalloproteinase-14 (*Mmp14*). Relative expression was expressed as fold vs. vehicle (PBS + DMSO)-treated cells. Data are presented as bars and individual samples with lines corresponding to the mean and standard error of the mean (SEM). Sample sizes, N = 3.

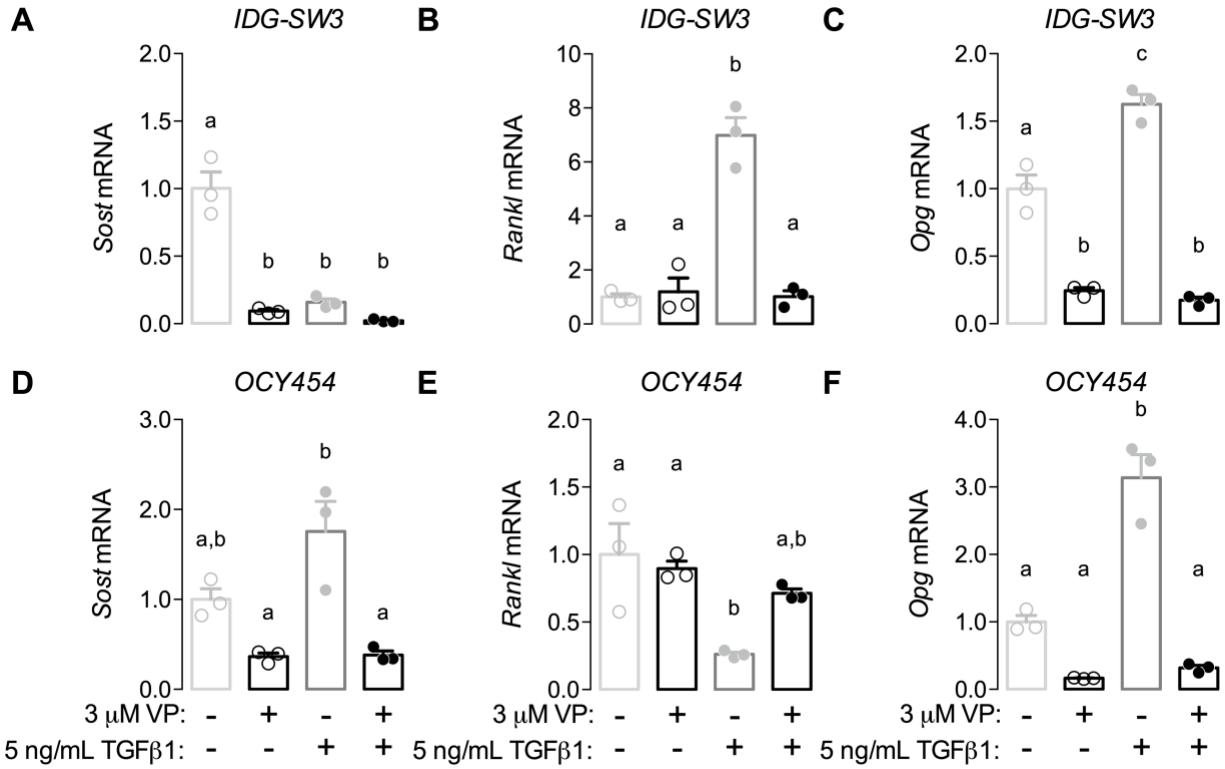

Supplemental Fig. 8. Combinatorial verteporfin (VP) and TGF-β treatment altered bone turnover-related gene expression *in vitro*. Osteocyte-like IDG-SW3 cells were differentiated for 21 days and combinatorially treated with inhibitor verteporfin (VP) and/or 5 ng/ml TGFβ1 at day 21. **A-C)** mRNA expression, normalized to *18S rRNA*, was evaluated for **(A)** sclerostin (*Sost*), **(B)** receptor activator of nuclear factor kappa-B ligand (*Rankl*), and **(C)** osteoprotegerin (*Opg*). Osteocyte-like cells, OCY454, were differentiated for 12 days. Cells were combinatorially treated with inhibitor verteporfin (VP) and 5 ng/ml TGF-β1 at day 12. **D-F)** mRNA expression, normalized to *18S rRNA*, was evaluated for **(D)** sclerostin (*Sost*), **(E)** receptor activator of nuclear factor kappa-B ligand (*Rankl*), and **(F)** osteoprotegerin (*Opg*). Relative expression was expressed as fold vs. vehicle (PBS + DMSO)-treated cells. Data are presented as bars and individual samples with lines corresponding to the mean and standard error of the mean (SEM). Sample sizes, N = 3.

Supplemental Table 1: qPCR primers. Mouse primers used for qPCR

Gene	Primer Sequence (5' to 3')	
18S rRNA	F R	CGAACGTCTGCCCTATCAAC GGCCTCGAAAGAGTCCTGTA
Yap	F R	TGGACGTGGAGTCTGTGTTG AAGCGGAACAACGATGGACA
Taz	F R	GTCCATCACTTCCACCTC TTGACGCATCCTAATCCT
Col1a1	F R	GCTCCTCTTAGGGGCCACT CCACGTCTCACCATTGGGG
Alp	F R	GGACAGGACACACACACACA CAAACAGGAGAGCCACTTCA
Ocn	F R	TGAGCTTAACCCTGCTTGTG TAGGGCAGCACAGGTCCTA
Bsp	F R	ACAATCCGTGCCACTCACT TTTCATCGAGAAAGCACAGG
Dmp1	F R	GAACAGTGAGTCATCAGAAG AAAGGTATCATCTCCACTGTC
Ctsk	F R	GAGGGCCAACTCAAGAAGAA GCCGTGGCGTTATACATACA
Mmp13	F R	CGGGAATCCTGAAGAAGTCTACA CTAAGCCAAAGAAAGATTGCATTTC
Mmp14	F R	AGGAGACGGAGGTGATCATCATTG GTCCCATGGCGTCTGAAGA
Sost	F R	TCCTCCTGAGAACAACCAGAC TGTCAGGAAGCGGGTGTAGTG
Phex	F R	TCATTGATACCAGACTCTACC CAATGGTTTTCTTCCTCTCG
Serpine1	F R	CAGATGACCACAGCGGGGAA GGCATGAGCTGTGCCCTTCT
Opg	F R	AGAGCAAACCTTCCAGCTGC CTGCTCTGTGGTGAGGTTCG
Rankl	F R	CCAAGATCTCTAACATGACG CACCATCGCTGAAGATAGT

Supplemental Table 2: Post-hoc power analyses. Power analyses for perilacunar/canalicular phenotypic results

Figure Panel	Parameter	Power
Figure 4C	Stiffness	0.99
Figure 5G	Canalicular length	0.99
Figure 6C	Branch length	0.95
Figure7B	Calcein+ lacunae	0.92
Figure 7C	*Col1a1* mRNA	0.74
Figure7E	CTSK+ lacunae	0.86
Figure 7F	*Ctsk* mRNA	0.96
Figure7H	MMP13+ lacunae	0.83
Figure 7I	*Mmp13* mRNA	0.99
Figure7K	MMP14+ lacunae	0.74
Figure 7L	*Mmp14* mRNA	0.83